

Optimal Social Limitation Reduction under Vaccination and Booster Doses

Paolo Di Giamberardino ^a and Daniela Iacoviello ^b

Department of Computer, Control and Management Engineering, Sapienza University of Rome, Rome, Italy

Keywords: Epidemic Modeling, COVID-19, Vaccination, Optimal Control, Social Behaviour.

Abstract: In the paper an optimal control solution is provided for the containment of the number of infected individuals in COVID-19 pandemic under vaccination campaign. The possibility to dynamically change the cost of the controls according to the ongoing evolution within the design procedure allows to get great efforts in presence of very serious disease conditions, saving resources otherwise. The different contribution of vaccinated and unvaccinated individuals to the epidemic spread is investigated, optimising the controls which describe the individual contact restrictions separately for the two classes and showing that it would have been possible to reduce all the social limitations introduced by many governments for the vaccinated individuals since the beginning of the vaccination campaign.

1 INTRODUCTION

COVID-19 is a sanitary emergency since January 2020 and the scientific community has started to study the evolution and the spread of the infection by means of mathematical models which had to follow the changes and the novelties in the knowledge of the illness, updated day by day, and in the possibility to fight the virus, as for examples (Di Giamberardino et al., 2021), (Giordano et al., 2020), (Tang et al., 2020), (Di Giamberardino and Iacoviello, 2021), (Radulescu et al., 2020). In particular, since the end of 2020, the availability of an effective vaccine makes it possible to introduce in all the models a new important control input, especially for the initial problem of scheduling the vaccinations among population categories. There is for example (Diagne et al., 2021), with the study of the efficacy of the vaccination with respect to the amount of population immunized.

There is a great relationship between the level of immunization of the population and the relax of the individual containment limitations. The necessity of a booster dose after the two doses cycle of vaccinations highly increased the people immunization, allowing to strongly reduce or even eliminate social restrictions in many places. Different control actions have been proposed in literature to reduce the number of infected patients; in particular, optimal control

allows to allocate efficiently the available limited resources, as in (Silva et al., 2021) referred in particular to the Portugal situation, where an optimal strategy is proposed to maximize the number of people that can return to normal life minimizing the number of infected patients, taking into account the level of hospitalization. In (Olivares and Staffetti, 2021) the effects of various vaccination strategies are studied considering realistic scenarios in which constraints on vaccine administration are introduced. Optimal solutions for vaccination strategies are also proposed improving existing models by the addition of compartments which take into account new knowledge on epidemic behaviour, like in (Liu et al., 2021) with the introduction of class of people for which the vaccine is ineffective.

In this paper, following the approach described in (Di Giamberardino and Iacoviello, 2017), it is proposed an optimal control obtained minimizing a suitable cost index in which the controls are weighted on the basis of the severity of the pandemic situation. In particular, this approach is used to act on the most invasive containment measure represented by the individual contact limitations with consequences on the everyday life and economy. A new mathematical model, which takes into account the possibility of a periodic reiteration with respect to the vaccination procedure, is here proposed as an improvement of previously adopted ones to better fit the present epidemic conditions.

^a  <https://orcid.org/0000-0002-9113-8608>

^b  <https://orcid.org/0000-0003-3506-1455>

The paper is organized as follows; in Section 2, the new mathematical model is introduced and then analysed in Section 3. In Section 4 the optimal control strategy is presented. Numerical results are shown in Section 5 and a discussion is provided in Section 6.

2 THE MATHEMATICAL MODEL

Since the beginning of 2021, the mathematical modelling of COVID-19 in a population can assume vaccination as a real possibility to contain virus spread. As long as information about vaccine efficacy, level of immunization and time of protection duration have been acquired, the possibility of a booster dose has to be introduced in any model; the number of categories, i.e. compartments, in the mathematical models must take into account the different level of vaccination, in addition to the different condition with respect to the disease. The model here adopted is based on a preliminary split into two main categories with respect to the vaccination conditions: those who have not received any vaccination dose and those who have started the vaccination cycle. The two groups are further particularized, depending to their specific condition with respect to the disease. For the population not vaccinated the well known *SEIR* model is chosen. A *SEIR*-like model is adopted also for the vaccinated population, but distinguishing the healthy subjects on the number of vaccination doses received: there is the class *P*, including those that have received only the first dose, the class *V* including the ones that have completed the vaccination cycle (second dose for two doses vaccine or unique dose for single dose ones), and the class *B*, containing the subjects that, after a full vaccination cycle or healed from infection, are losing immunity and are suggested to get the booster dose; they are not completely susceptible to the infection but the protection of the vaccine decreases with time and they can be infected with a course of the illness that could depend on the time elapsed since the completion of the vaccination cycle. This aspect is still under investigation by the researchers; in this paper we will assume that if a subject in *B* is infected he will have, probably, the same reaction to the virus as that of a subject in the *P* or *V* condition.

More precisely, the population is partitioned into 10 compartments:

- *S*: susceptible subjects, composed by the healthy part of the population which is not vaccinated yet;
- *E*: exposed individuals, i.e. the subjects in the incubation period; they are infected but can not infect;

- *I*: infected patients, that can infect the susceptible individuals and the subjects in *P* and *V* compartments;
- *R*: removed subjects, immunised by vaccination or because healed from the virus;
- *P*: healthy individuals that received the first vaccination dose;
- *V*: healthy subjects that received both the vaccination doses;
- *E_V*: exposed vaccinated individuals, i.e. the vaccinated subjects in the incubation period; as *E*, they are infected but cannot infect;
- *I_V*: vaccinated infected patients, that can infect both the susceptible non vaccinated individuals, but also the subjects in *P* and *V* compartments;
- *R_V*: removed vaccinated subjects;
- *B*: individuals which are losing immunization and then require a booster vaccine dose.

The dynamics describing the epidemic spread and its evolution can be written as

$$\dot{S} = N - \beta_{SI}(1 - u_S)SI - \beta_{SI_V}(1 - u_S)SI_V - d_S S - u_1 S - u_4 S \quad (1)$$

$$\dot{E} = \beta_{SI}(1 - u_S)SI + \beta_{SI_V}(1 - u_S)SI_V - d_E E - kE - u_1 E \quad (2)$$

$$\dot{I} = -d_I I + kE - \gamma_I I \quad (3)$$

$$\dot{R} = -d_R R + \gamma_I I - r_2 R - u_3 R \quad (4)$$

$$\dot{P} = -\beta_{PI}(1 - u_P)PI - \beta_{PI_V}(1 - u_P)PI_V - d_P P + u_1 S - u_2 P \quad (5)$$

$$\dot{V} = -\beta_{VI}(1 - u_V)VI - \beta_{VI_V}(1 - u_V)VI_V - d_V V - r_3 V + u_2 P + u_3 R + u_4 S + u_5 B \quad (6)$$

$$\begin{aligned} \dot{E}_V = & \beta_{VI}(1 - u_V)VI + \beta_{VI_V}(1 - u_V)VI_V \\ & + \beta_{PI}(1 - u_P)PI + \beta_{PI_V}(1 - u_P)PI_V \\ & + \beta_{BI}(1 - u_B)BI + \beta_{BI_V}(1 - u_B)BI_V \\ & - d_{E_V} E_V - kE_V + u_1 E \end{aligned} \quad (7)$$

$$\dot{I}_V = kE_V - d_{I_V} I_V - \gamma_V I_V \quad (8)$$

$$\dot{R}_V = -d_{R_V} R_V + \gamma_V I_V - r_1 R_V \quad (9)$$

$$\begin{aligned} \dot{B} = & r_2 R + r_1 R_V + r_3 V - u_5 B - d_B B \\ & - \beta_{BI}(1 - u_B)BI - \beta_{BI_V}(1 - u_B)BI_V \end{aligned} \quad (10)$$

The block diagram of the proposed model is shown in Fig.1 The controls u_i , $i = 1, \dots, 5$, denote the vaccination strategy. More precisely, a susceptible subject in *S* is vaccinated a first time with rate u_1 (with $u_1 S$ representing the daily number of doses administered) and then he receives the second dose after an average time $\frac{1}{u_2}$. An exposed subject in *E* is still not aware of being infected so, in a vaccination campaign he

deduced by evaluating the next generations matrix (Van Den Driessche, 2017); its calculus requires the study of the part of the system (11) involving the evolution of the subjects infected, in this case the individuals belonging to the classes E, I . The control actions (in our case the vaccination effort) are all set equal to zero. The reduced system involving the variables (E, I) and the corresponding variations (2), (3), may be written enhancing the contributions due to the infection, \mathcal{F} , and the ones due to changing the health condition, \mathcal{V} :

$$\begin{pmatrix} \dot{E} \\ \dot{I} \end{pmatrix} = \mathcal{F} - \mathcal{V} \quad (16)$$

where

$$\mathcal{F} = \begin{pmatrix} \beta_{SI}SI + \beta_{VI}SI_V \\ 0 \end{pmatrix} \quad (17)$$

$$\mathcal{V} = \begin{pmatrix} d_E E + kE \\ -kE + d_I I + \gamma I \end{pmatrix} \quad (18)$$

The variations of these matrices with respect to the variables E, I , evaluated in the disease free equilibrium point X^e , yield the matrices F and V respectively:

$$F = \left. \frac{\partial \mathcal{F}}{\partial (E, I)} \right|_{X^e} = \begin{pmatrix} 0 & \beta_{SI} \frac{N}{d_S} \\ 0 & 0 \end{pmatrix}, \quad (19)$$

and

$$V = \left. \frac{\partial \mathcal{V}}{\partial (E, I)} \right|_{X^e} = \begin{pmatrix} d_E + k & 0 \\ -k & d_I + \gamma \end{pmatrix} \quad (20)$$

Under these positions, the reproduction number \mathcal{R}_0 is given by the dominant eigenvalue of the next generation matrix

$$FV^{-1} = \begin{pmatrix} \frac{k\beta_{SI}N}{d_S(d_E+k)(d_I+\gamma)} & \frac{\beta_{SI}N}{d_S(d_I+\gamma)} \\ 0 & 0 \end{pmatrix} \quad (21)$$

Then, the basic reproduction number \mathcal{R}_0 is obtained from the non-null eigenvalue and is given by

$$\mathcal{R}_0 = \frac{k\beta_{SI}N}{d_S(d_E+k)(d_I+\gamma)} \quad (22)$$

By comparison of this expression (22) with the stability condition (15), the known relationships between the epidemiological and stability characteristics of the system is remarked: the epidemics tends to extinguish if $\mathcal{R}_0 < 1$, so that the condition can be written as

$$\frac{k\beta_{SI}N}{d_S(d_E+k)(d_I+\gamma)} < 1 \quad (23)$$

that can be rearranged as (15).

4 DEFINITION OF THE OPTIMAL CONTROL PROBLEM FOR BEST STRATEGY

Since the beginning of 2021, the availability of vaccinations added an important, and hopefully definitive, action to the previous *non pharmaceutical* ones which have always represented a freedom limitation of individuals.

The proposed study aims at evaluating, in an optimal control framework, the possibility and the optimal time of relaxing the contact limitations between individuals and the constraints on the use of protective devices under a full vaccination campaign. The general cost function should consider time, state and controls. For sake of clarity in the following discussion, simple but effective choices are performed. The state considered in the minimization are the two meaningful for evaluating the epidemic spread, the two infected classes $I(t)$ and $I_V(t)$; the controls representing the vaccinations are set constant under the hypothesis of a full rate vaccination while the ones denoting the contact limitations are part of the control to be defined. Due to their significant differences in terms of infection spread contributions, the unvaccinated individuals and the vaccinated ones are maintained different, so that the two controls u_S and u_V are kept distinguished; in view of a realistic correspondence with social behaviour, people with one dose only is considered as unvaccinated, that is $u_P = u_S$, while the class of people requiring the booster dose is considered equivalent to the vaccinated ones: $u_B = u_V$.

The design approach here followed is the same as the one introduced in (Di Giamberardino and Iacoviello, 2017): the control is weighted by a function of the current state, so that different costs can be associated to different dangerousness levels of the epidemics effects. Under the choice of $I(t)$ and $I_V(t)$ as the most meaningful ones, the weights are defined as functions of these two state variables only.

Under the present choices, the cost function is

$$J(U, T) = \int_0^T (K_1 + K_2 I(t) + K_3 I_V(t) + \frac{1}{2} (W_S u_S^2(t) + W_V u_V^2(t))) dt \quad (24)$$

with $W_S = W_S(I(t), I_V(t))$ and $W_V = W_V(I(t), I_V(t))$ to be defined according to the severity of the spread and the population health situation. This can be reformulated as the necessity of a stronger intervention under higher number of infected patients, $I(t)$ and $I_V(t)$

The controls are chosen bounded to consider logistic, economic, technical and physical constraints,

so that $U_{Sm} \leq u_S(t) \leq U_{SM}$ and $U_{Vm} \leq u_V(t) \leq U_{VM}$; according to the optimal control problem formulation, such bounds yield to the constraints formulation

$$\begin{cases} q_1(t) = U_{SM} - u_S(t) < 0 \\ q_2(t) = u_S(t) - U_{Sm} < 0 \\ q_3(t) = U_{VM} - u_V(t) < 0 \\ q_4(t) = u_V(t) - U_{Vm} < 0 \end{cases} \quad (25)$$

For the definition of the weight function $W_i(I(t), I_V(t))$, a Cartesian decomposition of the subspace $\mathfrak{R}^2 = I \times I_V$ of the state space is performed. The domain interval $[0, +\infty]$, in which the number of infected non-vaccinated patients, $I(t)$, can vary, is partitioned into $n_1 + 1$ subintervals $[I_i, I_{i+1})$, $i = 0, \dots, n_1$, with $I_0 = 0$, $I_1 = I_m$, and $I_{n_1+1} = +\infty$; the same is performed for $I_V(t)$: its domain definition $[0, +\infty]$ is partitioned into $n_2 + 1$ subintervals $[I_{V,i}, I_{V,i+1})$, $i = 0, \dots, n_2$, with $I_{V,0} = 0$, $I_{V,1} = I_{Vm}$, and $I_{V,n_2+1} = +\infty$. The weight function chosen $W_i(I(t), I_V(t))$ for the control in the cost index aims at improving the control effort in case of severe epidemiological situation, while relaxing the measures or even cancelling any containment action when the number of infected patients is low. The values I_m and I_{Vm} represent the minimum number of infected non vaccinated and vaccinate patients, respectively, below which any control action is no more motivated.

For the control u_S it is assumed that, when $I(t) \in [I_i, I_{i+1})$ and $I_V(t) \in [I_{V,j}, I_{V,j+1})$, the weight is constant and set equal to a certain value $\alpha_{i,j}^S$, chosen so that the higher is the severity of the disease, the lower is the cost of the control action. The same is performed for the control u_V . So, defining $I_{i,j} = [I_i, I_{i+1}) \times [I_{V,j}, I_{V,j+1})$, one has

$$W_h(I(t), I_V(t)) = \alpha_{i,j}^h \text{ for } (I(t), I_V(t)) \in I_{i,j} \quad (26)$$

with $\alpha_{i,j}^h \in R_+$, $i = 1, \dots, n_1$, $j = 1, \dots, n_2$, $h \in \{S, V\}$. For their meanings, one has

$$\alpha_{i,j}^h \leq \alpha_{i+1,j}^h \quad (27)$$

$$\alpha_{i,j}^h \leq \alpha_{i,j+1}^h \quad (28)$$

$$\alpha_{i,j}^h < \alpha_{i+1,j+1}^h \quad (29)$$

The control is not applied, and hence not defined, when $(I(t), I_V(t)) \in I_{0,0}$.

The piecewise definition of the weight functions W can be formulated as a decomposition over each interval $I_{i,j}$ of a constant weighted optimal control problem. With the choice of the cost index (24), it follows that when the number of infected non-vaccinated patients $I(t)$ falls in the interval $[I_i, I_{i+1})$ and the number of infected vaccinated patients falls in the interval

$[I_{V,j}, I_{V,j+1})$, the Hamiltonian can be defined as

$$H(X, U, \lambda) = K_1 + K_2 I(t) + K_3 I_V(t) + \frac{1}{2} \alpha_{i,j}^S u_S^2(t) + \frac{1}{2} \alpha_{i,j}^V u_V^2(t) + \lambda^T(t) F(X, U) \quad (30)$$

with λ the 10-dimension costate function. Note that, obviously, the Hamiltonian and the costate functions depend on the specific interval $[I_i, I_{i+1}) \times [I_{V,j}, I_{V,j+1})$; to avoid weighing down the notation, the subscript i, j are not written.

The solution follows an iterative computation. Starting from the initial condition, the first interval $I_{i,j}$ is defined with $I(0) \in [I_i, I_{i+1})$ and $I_V(0) \in [I_{V,j}, I_{V,j+1})$. If $i \neq 0$ and $j \neq 0$, the optimal control problem can be posed, with $W_S(I(t), I_V(t)) = \alpha_{i,j}^S$ and $W_V(I(t), I_V(t)) = \alpha_{i,j}^V$ used in the Hamiltonian (30), along with all the boundary conditions and constraints, for getting the optimal solution $(X(t), \lambda(t), U(t))$. This is the optimal solution until $(I(t), I_V(t)) \in I_{i,j}$. Along the solution, at the first time \bar{t}_1 in which the number of infected people $I(\bar{t}_1)$ and/or $I_V(\bar{t}_1)$ crosses upper or lower boundary values of the domain $I_{i,j}$ a switch occurs since at least one of the functions $W_i(I(t), I_V(t))$ changes its value; a new optimal control problem must be defined and then solved in the new region; the Hamiltonian is defined as in (30) but with

$$\begin{aligned} W_S(I(t), I_V(t)) &= \alpha_{i-1,j}^S \text{ if } (I(\bar{t}_1^+), I_V(\bar{t}_1^+)) \in I_{i-1,j} \\ W_S(I(t), I_V(t)) &= \alpha_{i+1,j}^S \text{ if } (I(\bar{t}_1^+), I_V(\bar{t}_1^+)) \in I_{i+1,j} \\ W_S(I(t), I_V(t)) &= \alpha_{i,j-1}^S \text{ if } (I(\bar{t}_1^+), I_V(\bar{t}_1^+)) \in I_{i,j-1} \\ W_S(I(t), I_V(t)) &= \alpha_{i,j+1}^S \text{ if } (I(\bar{t}_1^+), I_V(\bar{t}_1^+)) \in I_{i,j+1} \\ W_S(I(t), I_V(t)) &= \alpha_{i-1,j-1}^S \text{ if } (I(\bar{t}_1^+), I_V(\bar{t}_1^+)) \in I_{i-1,j-1} \\ W_S(I(t), I_V(t)) &= \alpha_{i+1,j+1}^S \text{ if } (I(\bar{t}_1^+), I_V(\bar{t}_1^+)) \in I_{i+1,j+1} \\ W_S(I(t), I_V(t)) &= \alpha_{i-1,j+1}^S \text{ if } (I(\bar{t}_1^+), I_V(\bar{t}_1^+)) \in I_{i-1,j+1} \\ W_S(I(t), I_V(t)) &= \alpha_{i+1,j-1}^S \text{ if } (I(\bar{t}_1^+), I_V(\bar{t}_1^+)) \in I_{i+1,j-1} \end{aligned}$$

and, equivalently, for the weight $W_V(I(t), I_V(t))$. The bounds crossed and the update of the values for the case of $W_V(I(t), I_V(t)) = \alpha_{i,j}^V$ are depicted in Figure 2.

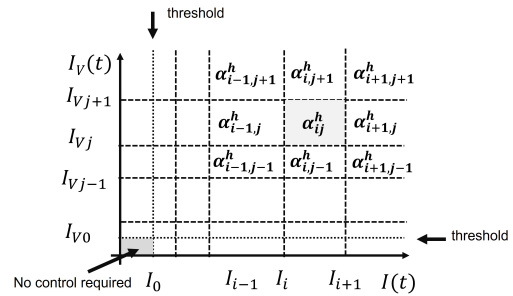


Figure 2: Procedure to change the weights in the cost function J .

The first segment of the optimal solution defined over the time interval $[0, \bar{t}_1]$ is then obtained. Taking

the initial time \bar{t}_1 and the initial conditions $X(\bar{t}_1)$, a new optimal control problem is then defined, different from the previous one for the choices of the weight coefficients of the control only. According to the same procedure, a new switching instant \bar{t}_2 can be found, and so on.

A final time T can be fixed (and then $K_1 = 0$ in (30)) or left free. In the first case, it may happen that there is a switching instant $\bar{t}_s < T$ such that the state evolution enters the $I_{0,0}$ region. In this case, the actual final time is no more T but \bar{t}_s . In the second case, \bar{t}_s is the final time to be computed. Note that the actual final time \bar{t}_s cannot be assured a priori, even if T is defined, since its value depends on the state evolution.

For each iteration, the necessary condition of the Pontryagin principle to solve the optimal control problem over each interval can be written as follows, starting from the costate equations

$$\dot{\lambda} = \frac{\partial H}{\partial X} \Big|_T$$

where $\lambda(t)$ has the first order derivative continuous almost everywhere and $\lambda(T) = 0$.

The Pontryagin inequality yields for the two controls $u_S(t)$ and $u_V(t)$

$$\frac{1}{2} \alpha_{ij}^S u_S^2 + \Gamma_S u_S \leq \frac{1}{2} \alpha_{ij}^S \omega_S^2 + \Gamma_S \omega_S \quad (31)$$

$$\frac{1}{2} \alpha_{ij}^V u_V^2 + \Gamma_V u_V \leq \frac{1}{2} \alpha_{ij}^V \omega_V^2 + \Gamma_V \omega_V \quad (32)$$

where

$$\Gamma_S = (\lambda_1 - \lambda_2)(\beta_{SI}SI + \beta_{SI_V}SI_V) \quad (33)$$

$$\Gamma_V = (\lambda_6 - \lambda_7)(\beta_{VI}VI + \beta_{VI_V}VI_V) \quad (34)$$

and the ω_S and ω_V represent any admissible control, that is any control function satisfying (25).

Due to the convexity, with respect to u_S , of the function $\frac{1}{2} \alpha_{ij}^S u_S^2 + \Gamma_S u_S$, and the same for the control u_V , the inequalities (31) and (32) yield

$$u_S = \min \left\{ U_{SM}, \max \left\{ U_{Sm}, \frac{-\Gamma_S}{\alpha_{ij}^S} \right\} \right\} \quad (35)$$

$$u_V = \min \left\{ U_{VM}, \max \left\{ U_{Vm}, \frac{-\Gamma_V}{\alpha_{ij}^V} \right\} \right\} \quad (36)$$

The complete optimal control is obtained as the concatenation of the controls obtained in each single step.

In next Section 5, a numerical case is illustrated within the proposed optimal control design framework, defining the optimal switching approaches to social contact limitations as a consequence of a massive vaccination campaign. The idea is to show how

the present approach can reproduce the political decisions on increasing or decreasing, at certain times according to the epidemic spread, the social containment constraints; moreover, evidencing the lower contribution of vaccinated individuals to the epidemic spread with respect to the not vaccinated ones, and the different impact in terms of public health and hospital occupancy, the optimal solutions show that different policies for unvaccinated and vaccinated individuals can be adopted.

For this particular problem, a set of assumptions and simplifications are introduced. The vaccinations are assumed to proceed at a constant rate, the one admissible by the sanitary systems, following the idea that the entire population aims at being vaccinated; the contact rate limitation for people vaccinated with the first dose only, P , is assumed the same as for the ones not yet vaccinated, S , so that $u_P = u_S$. A further simplification, not far from reality especially in more recent times, is to neglect the single dose vaccine usage, so setting $u_4 = 0$.

5 NUMERICAL RESULTS

In this Section, the switching optimal control approach described in Section 4 is used to generate the optimal social and individual distancing, specific for non vaccinated and vaccinated individuals, modulated according to different level of severity of the epidemic measured on the basis of the infected individuals, both among susceptibles and vaccinated ones. With respect to the cost function (24), the following coefficients are taken:

$$K_1 = 10; \quad K_2 = 10; \quad K_3 = 1 \quad (37)$$

The decomposition of the subspace $I \times I_V$ is performed assuming $n_1 = n_2 = 4$ and, for each of the two components, the subinterval thresholds

$$I_1 = I_{V,1} = 5 \cdot 10^4, \quad I_2 = I_{V,2} = 10^6, \quad I_3 = I_{V,3} = 3 \cdot 10^6 \quad (38)$$

The corresponding $n_1 \times n_2$ weight matrices α^S and α^V are chosen as

$$\alpha^S = \alpha^V = \begin{pmatrix} 10^{10} & 10^8 & 10^7 & 10^6 \\ 10^8 & 10^7 & 10^6 & 10^5 \\ 10^7 & 10^6 & 10^4 & 10^3 \\ 10^6 & 10^5 & 10^3 & 10 \end{pmatrix} \quad (39)$$

An important choice concerns the transmission rates $\beta_{*,*}$. Taken $\beta_{SI} = 10^{-8}$ as an average value from literature (Di Giambardino et al., 2021), (Dan et al., 2021) and (Diagne et al., 2021), the other rates are chosen as

$$\begin{aligned} \beta_{SI_V} &= 0.1\beta_{SI}; & \beta_{PI} &= 0.8\beta_{SI}; \\ \beta_{PI_V} &= 0.2\beta_{SI}; & \beta_{VI} &= 0.1\beta_{SI}; \\ \beta_{VI_V} &= 0.02\beta_{SI}; & \beta_{BI} &= 0.01\beta_{SI}; \\ \beta_{BI_V} &= 0.005\beta_{SI} \end{aligned} \quad (40)$$

The death rates in model (1)–(10) are the same for all the compartments except for the infected ones, for which it results higher than the other ones. Values adopted are

$$\begin{aligned} d_S = d_E = d_V = d_{E_V} = d_R = d_P = \\ = d_{R_V} = d_B = 2.81 \cdot 10^{-5} \end{aligned} \quad (41)$$

and

$$d_I = 5 \cdot 10^{-3}, \quad d_{I_V} = 0.1 * d_I \quad (42)$$

For the remaining parameters, the values are assumed from assessed knowledge on time constant of illness progression:

$$r_1 = r_2 = r_3 = \frac{1}{270}; \quad k = \frac{1}{4}; \quad \gamma_V = \gamma_I = \frac{1}{21}; \quad (43)$$

Tables 1 and 2 summarise the values assumed for the parameter

Table 1: Values of parameters assumed in numerical simulations.

Parameter	Value
N	1.69e3
r_1, r_2, r_3	1/270
k	1/4
γ_I, γ_V	1/21
$d_S, d_E, d_V, d_{E_V}, d_R, d_P, d_{R_V}, d_B$	2.81e-5
d_I	5e-3
d_{I_V}	0.1d _I

Table 2: Values of the transmission rates β_* .

Parameter	Value
β_{SI}	1e-8
β_{SI_V}	0.1 β_{SI}
β_{PI}	0.8 β_{SI}
β_{PI_V}	0.2 β_{SI}
β_{VI}	0.1 β_{SI}
β_{VI_V}	0.02 β_{SI}
β_{BI}	0.01 β_{SI}
β_{BI_V}	0.005 β_{SI}

The controls u_S and u_V are the ones that has to be optimised. As far as the other seven is concerned, the following assumptions are made. First of all, the remaining containment controls u_P and u_B are taken, as previously said, equal to u_S and u_V respectively. The choice is mainly motivated by the fact that it is very difficult to impose different everyday life behaviour to people in slightly similar conditions with respect to vaccination. Moreover, according to the previous discussions, the vaccination rates are assumed constant over the simulation time; their values are $u_1 = 0.01$, $u_2 = 1/21$, $u_3 = 0$, $u_4 = 0.1u_1$ and $u_5 = 1/120$. To complete the problem set up, the values assumed for the constraints (25) are $U_{SM} = U_{VM} = 0.95$ and $U_{Sm} = U_{Vm} = 0$.

Simulation is performed to replicate the situation in Italy from the beginning of massive vaccination on January 2021. The goal is to put in evidence how it would have been possible to relax the containment measures acting since the earliest times, differently according to vaccination conditions. The first four months have been considered.

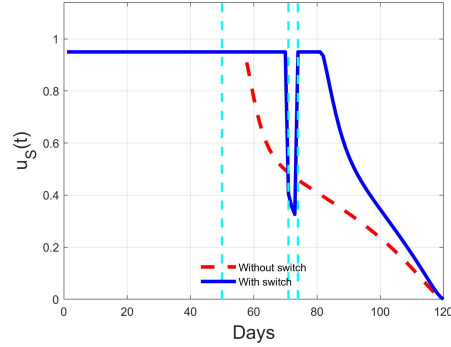


Figure 3: Optimal switching control $u_S(t)$ (solid blue line) compared with a non switching solution (dashed red line).

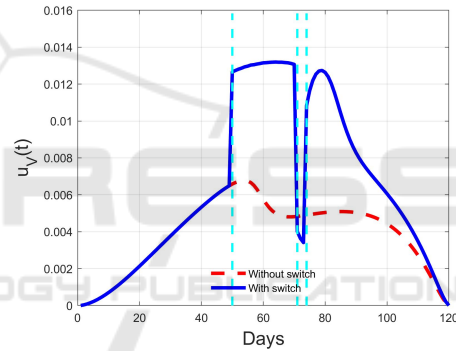


Figure 4: Optimal switching control $u_V(t)$ (solid blue line) compared with a non switching solution (dashed red line).

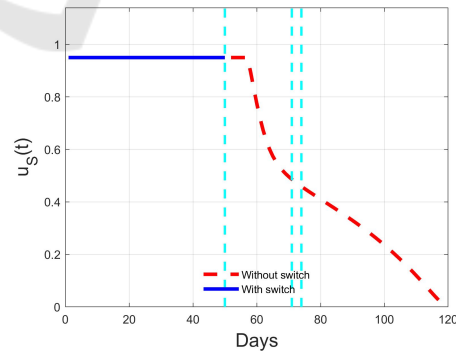


Figure 5: Optimal switching control $u_S(t)$ over the first time interval (solid blue line) and the remaining part without switch (dashed red line).

The resulting optimal switching controls are plotted in Figures 3 and 4 for $u_S(t)$ and $u_V(t)$ respectively, while the sequences of control segments computed in the iterative procedure are reported in Figures 5–8 for

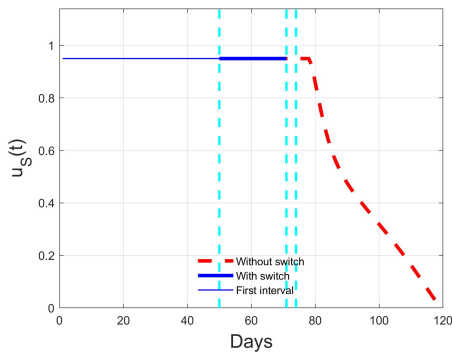


Figure 6: Optimal switching control $u_S(t)$ over the first two time intervals (thin and thick solid blue line) and the remaining part without switch (dashed red line).

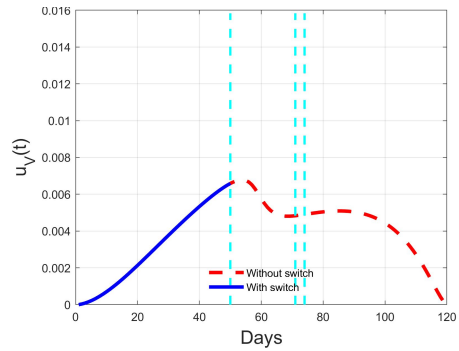


Figure 9: Optimal switching control $u_V(t)$ over the first time interval (solid blue line) and the remaining part without switch (dashed red line).

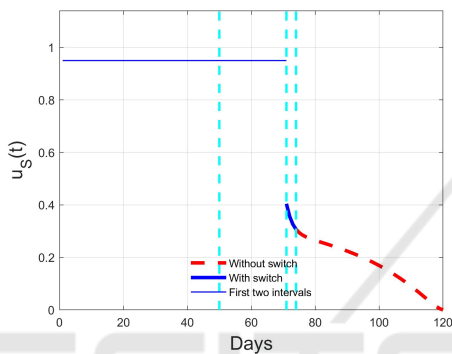


Figure 7: Optimal switching control $u_S(t)$ over the first three time intervals (thin and thick solid blue line) and the remaining part without switch (dashed red line).

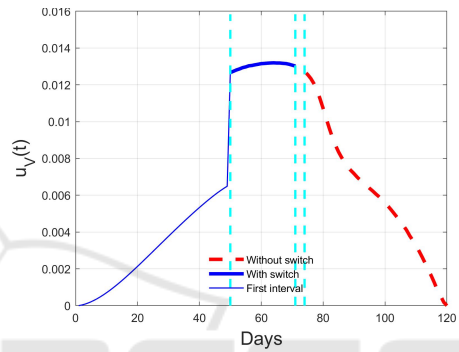


Figure 10: Optimal switching control $u_V(t)$ over the first two time intervals (thin and thick solid blue line) and the remaining part without switch (dashed red line).

$u_S(t)$ and in Figures 9 for $u_V(t)$.

The control design procedure is reported step by step. In Figures 3 and 4 the full optimal controls are reported as solid blue lines, showing the time switch instants $(\bar{t}_1, \bar{t}_2, \bar{t}_3) = (50, 71, 74)$. In the same figure, the switching solution is compared with the optimal one obtained keeping the weights W_S and W_V constant over all the integration (dashed red lines).

The above described iterative procedure is put in

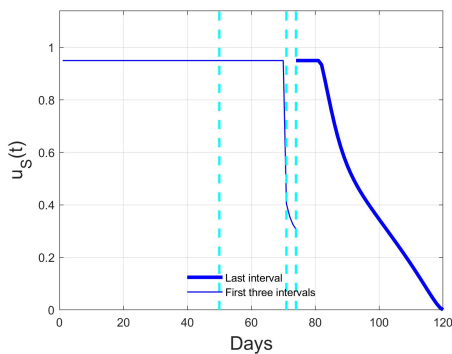


Figure 8: Optimal switching control $u_S(t)$: thin solid blue line for the already computed segments, thick solid blue line for the last segment.

evidence by the sequences of picture. Starting from Figures 5 and 9, the solutions of the first optimal problem are reported and the corresponding evolutions for $I(t)$ and $I_V(t)$ are depicted in Figures 13 and Figures 17. They correspond to the final optimal solution for the time interval $[0, 50]$, evidenced in the Figures, since at time $\bar{t}_1 = 50$ a switch occurs due to the passage of $I_V(t)$ from one region to the one above. The red dashed lines in these figures represent the evolution if the switch were not applied. Actually, with the

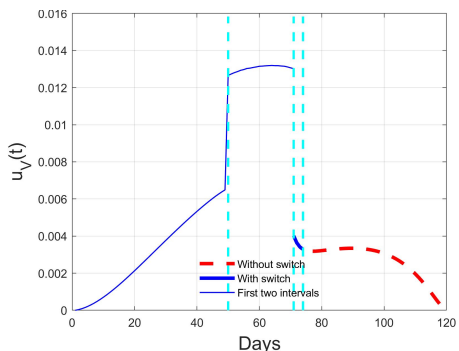


Figure 11: Optimal switching control $u_V(t)$ over the first three time intervals (thin and thick solid blue line) and the remaining part without switch (dashed red line).

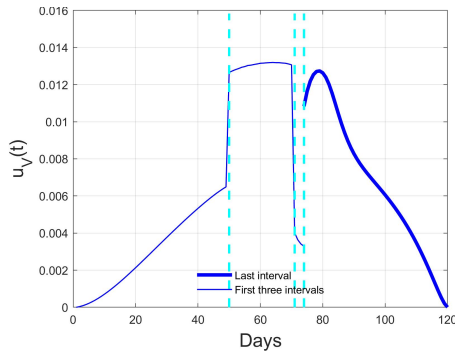


Figure 12: Optimal switching control $u_V(t)$: thin solid blue line for the already computed segments, thick solid blue line) for the last segment.

change of region, the new optimal problem is solved with different weights for the controls, in particular smaller than in the previous case due to the more dangerous situation of a greater number of infected individuals above the fixed threshold.

Figures 6 and 10 show the result of this latter problem, with the new optimal control depicted from $t = 50$ to the end. The segment computed in the previous step is marked with a thin blue line, the present segment with a thick blue line and the red dashed line denotes the remaining part of the solution if a new switch were not present. The corresponding effect on the optimal state evolution is reported in Figures 14 and 18 for the two classes of infected individuals. It can be noted that the introduction of changes in the weights of the cost function allow to react to a worse situation with a greater control effort.

At time $\bar{t}_3 = 74$ the higher control action brings the state variable $I_V(t)$ to return into the previous, less dangerous, region of decomposition, so giving a new switch with a consequent increment of the weights for the control in the cost function. The segment of controls in the time interval $[\bar{t}_2, \bar{t}_3) = [71, 74)$ are evidenced by thick blue solid curves in Figures 7 and 11 ($u_S(t)$ and $u_V(t)$ respectively), while the corresponding evolutions of $I(t)$ and $I_V(t)$ are reported in Figures 15 and 19, with the same notation as for the previous segment. The reduction of the controls effort after \bar{t}_2 produces an increment of infected individuals once more. This brings to a new switch in $t = \bar{t}_3$ and the consequent evolution over the last time segment considered. Figures 8 and 12 report the evolution in such a time interval for the controls, while Figure 16 and 20 depict the resulting time histories for $I(t)$ and $I_V(t)$.

6 CONCLUSIONS

In the present paper an optimal control approach with an available effort planned on the basis of the danger-

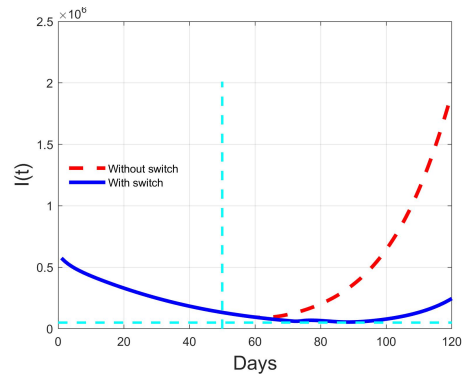


Figure 13: $I(t)$ evolution under optimal switching control (blue solid line) compared with the non switching solution (red dashed line).

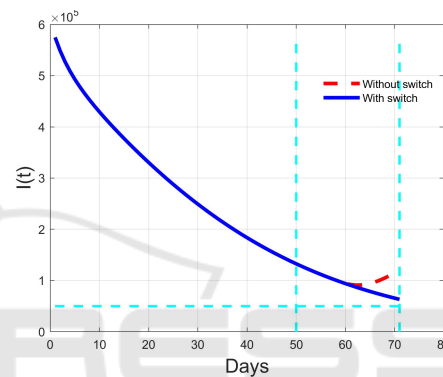


Figure 14: Switching (blue solid line) and non switching (red dashed line) evolution of $I(t)$ during the first two time intervals of the algorithm $[0,50)$ and $[50,71)$.

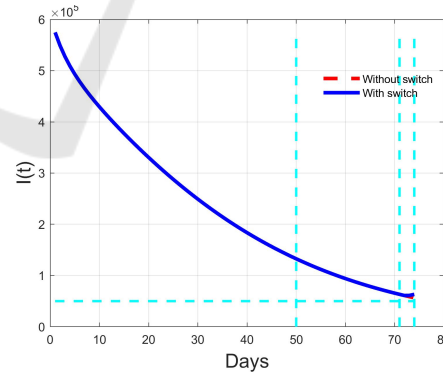


Figure 15: Comparison between switching (blue solid line) and non switching (red dashed line) evolution of $I(t)$ during the third time interval $[71,74)$.

ousness of the health conditions is proposed for defining the individual and social contact limitations after vaccination in COVID-19 pandemic situation. The results show how the possibility of allowing a greater, even more expensive, effort in some severe conditions while planning a reduction under less serious situations allow to have effective results with a global con-

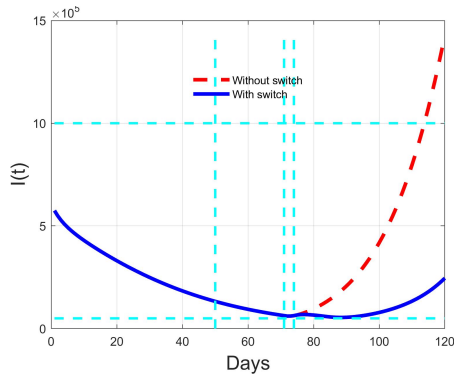


Figure 16: Comparison between switching (blue solid line) and non switching (red dashed line) evolution of $I(t)$ during the fourth time interval [74,120).

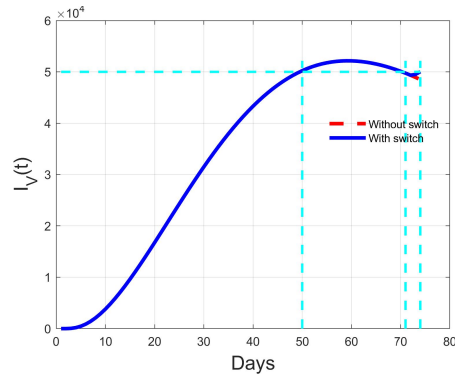


Figure 19: Comparison between switching (blue solid line) and non switching (red dashed line) evolution of $I_V(t)$ during the third time interval [71,74).

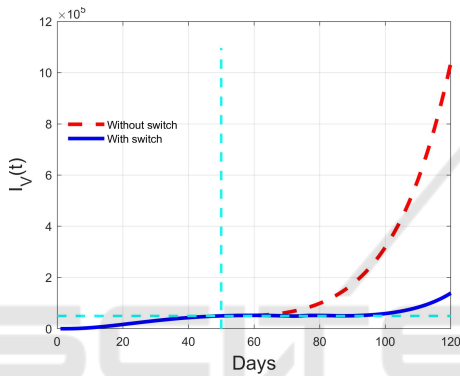


Figure 17: $I_V(t)$ evolution under optimal switching control (blue solid line) compared with the non switching solution (red dashed line).

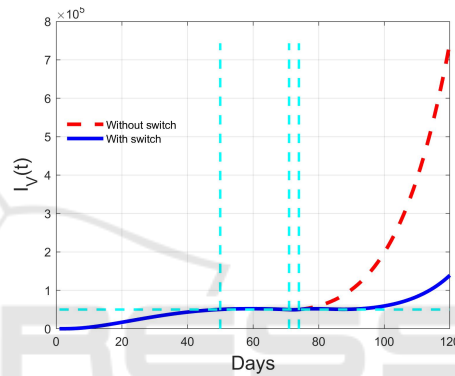


Figure 20: Comparison between switching (blue solid line) and non switching (red dashed line) evolution of $I(t)$ during the fourth time interval [74,120).

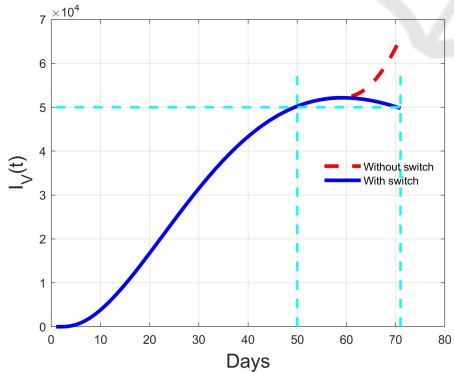


Figure 18: Switching (blue solid line) and non switching (red dashed line) evolution of $I_V(t)$ during the first two time intervals of the algorithm [0,50) and [50,71).

tainment of the resources and the costs. In particular, it has been shown how the restrictions on vaccinated and not vaccinated individuals would have been distinguished, reducing them for vaccinated ones since the beginning of the vaccination campaign. Actually, the use of specific certifications for entering restaurants, theatres and, generally, attending public events

with high number of participants, adopted in many countries, is supported by these results.

REFERENCES

Dan, J. M., Mateus, J., Kato, Y., Hastie, K., Yu, E. D., and Faliti, C. E. (2021). Immunological memory to sars-cov-2 assessed for up to 8 months after infection. *Science*, 371(6529):1–15.

Di Giamberardino, P. and Iacoviello, D. (2017). Optimal control of SIR epidemic model with state dependent switching cost index. *Biomedical Signal Processing and Control*, 31.

Di Giamberardino, P. and Iacoviello, D. (2020). A control based mathematical model for the evaluation of intervention line in epidemic spreads without vaccination: the covid-19 case study. *Submitted to IEEE Journal of Biomedical and Health Informatics*.

Di Giamberardino, P. and Iacoviello, D. (2021). Evaluation of the effect of different policies in the containment of epidemic spreads for the COVID-19 case. *Biomedical signal processing and control*, 65(102325):1–15.

- Di Giamberardino, P., Iacoviello, D., F.Papa, and C.Sinisgalli (2021). Dynamical evolution of COVID-19 in Italy with an evaluation of the size of the asymptomatic infective population. *IEEE Journal of Biomedical and Health Informatics*, 25(4):1326–1332.
- Diagne, M. L., Rwezaura, H., Tchoumi, S. Y., and Tchuenche, J. M. (2021). A mathematical model of covid-19 with vaccination and treatment. *Computational and Mathematical Methods in Medicine*, (1250129):1–16.
- Giordano, G., Blanchini, F., Bruno, R., Colaneri, P., Filippino, A. D., and Colaneri, M. (2020). Modeling the COVID-19 epidemic and implementation of population wide interventions in Italy. *Nature Medicine*, 26.
- Liu, Z., Omayrat, M., and Stursberg, O. (2021). A study on model-based optimization of vaccination strategies against epidemic virus spread. In *Proceedings of the 18th International Conference on Informatics in Control, Automation and Robotics - ICINCO*, pages 630–637. INSTICC, SciTePress.
- Olivares, A. and Staffetti, E. (2021). Optimal control-based vaccination and testing strategies for covid-19. *Computer Methods and Programs in Biomedicine*, 211(106411):1–9.
- Radulescu, A., Williams, C., and Cavanagh, K. (2020). Management strategies in a SEIR-type model of COVID-19 community spread. *Nature. Scientific Reports*, 21256.
- Silva, C. J., Cruz, C., Torres, D. F. M., Munuzuri, A. P., Carballosa, A., Area, I., Nieto, J. J., Pinto, R. F., Pasadouro, R., dos Santos, E., Abreu, W., and Mira, J. (2021). Optimal control of the covid-19 pandemic: controlled sanitary deconfinement in portugal. *Scientific Reports*, 11(3451):1–15.
- Tang, B., Bragazzi, N. L., Li, Q., Tang, S., Xiao, Y., and Wu, J. (2020). An updated estimation of the risk of transmission of the novel coronavirus (2019-nCov). *Infectious disease modeling*, 5.
- Van Den Driessche, P. (2017). Reproduction numbers of infectious disease models. *Infectious disease models*, 2:288–303.